

1 **Columbitization of fluorcalciopyrochlore by hydrothermalism at the**
2 **Saint-Honoré alkaline complex, Québec (Canada): new insights on**
3 **halite in carbonatites**

4
5 **Jonathan Tremblay^{1,a}, L. Paul Bédard¹, Guillaume Matton²**

6 ¹ *Sciences de la Terre, Université du Québec à Chicoutimi (UQAC), Chicoutimi, Québec (Canada), G7H*
7 *2B1*

8 ² *Niobec Inc., Saint-Honoré, Québec (Canada), G0V 1L0*

9 ^a *Corresponding author: Jonathan.tremblay11@uqac.ca*

10
11 **Abstract**

12 Niobium (Nb) in carbonatite is mainly hosted in fluorcalciopyrochlore and columbite-(Fe).
13 Information related to Nb petrogenesis is useful for understanding the processes related to
14 Nb mineralization and carbonatite evolution. The Saint-Honoré, Quebec, alkaline complex
15 offers a rare opportunity for studying these processes as the complex is not affected by
16 post-emplacement deformation, metamorphism nor weathering. Columbite-(Fe) is shown
17 to be an alteration product of fluorcalciopyrochlore (columbitization). Columbitization is
18 characterized by the leaching of Na and F from the A- and Y-sites of the pyrochlore crystal
19 structure. As alteration increases, Fe and Mn are slowly introduced while Ca is
20 simultaneously leached. Leached Ca and F then crystallize as inclusions of calcite and
21 fluorite within the columbite-(Fe). A-site cations and vacancies in the crystal structure of
22 fresh and altered pyrochlores demonstrate that pyrochlore alteration is hydrothermal in
23 origin. Moreover, halite is a ubiquitous mineral in the Saint-Honoré alkaline complex.
24 Petrographic evidence shows that halite forms in weakly altered pyrochlores, suggesting
25 halite has a secondary origin. As alteration increases, halite is expelled by the hydrothermal

26 fluid and is carried farther into the complex, filling fractures throughout the carbonatite. The
27 hydrothermal hypothesis is strengthened by significant enrichments in Cl and HREEs in
28 columbite-(Fe). Chlorine is most likely introduced by a hydrothermal fluid that increases
29 the solubility of REEs. A HREE rim is observed around magmatic apatite associated with
30 fluorcalciopyrochlore and columbite-(Fe), suggesting a late magmatic event related to
31 hydrothermal activity.

32

33 **Keywords**

34 Pyrochlore; Columbite-(Fe); Halite; Niobium; Carbonatite; Saint-Honoré

35

36 **1. Introduction**

37 Carbonatites are important rocks for understanding the Earth's evolution as they provide a
38 window into the mantle and its dynamics. As such, they have been abundantly studied
39 (Chakhmouradian et al., 2015; Decrée et al., 2015; Le Bas, 1981; Mitchell, 2015; Wyllie,
40 1966; among many others). However, the crustal evolution of carbonatites, either by
41 fractional crystallization, hydrothermalism, carbothermalism or weathering can obliterate
42 or modify much of the initial information recorded by these rocks. Thus, an understanding
43 of the evolution of carbonatites is essential to better constrain any interpretation of their
44 formation. Moreover, carbonatites are important economic rocks as they host strategic
45 metals such as rare earth elements (REEs) (Chakhmouradian and Wall, 2012; Giebel et al.
46 2017), niobium (Mariano, 1989; Wall et al., 1999) and, in some cases, base metals (e.g.
47 Cu; Heinrich, 1970). A rapidly increasing demand for Nb (Roskill, 2017) in emerging
48 countries (Mackay and Simandl, 2014), requires a better understanding of the
49 mineralization processes within carbonatites to develop avenues of possible exploration.

50 The petrography and chemistry of columbite and pyrochlore are often key for
51 understanding the genesis of Nb mineralization.

52

53 Within carbonatites, minerals from the pyrochlore group host Nb mineralization and act as
54 recorders of carbonatite petrogenesis (Atencio et al., 2010; Hogarth et al., 2000; Lumpkin
55 and Ewing, 1995). The pyrochlore mineral group contains more than a dozen species
56 although fluorcalciopyrochlore [(Ca,Na)₂(Nb,Ti)₂O₆(O,OH,F)] (Hogarth, 1977) is the end-
57 member that is usually exploited for Nb. A second economically important mineral in
58 carbonatite is columbite-(Fe) [(Fe,Mn)(Nb,Ti)₂O₆]. Columbite is generally found as a
59 primary mineral in granites and pegmatites (e.g. Cerný, 1989; Lumpkin, 1998). It is
60 generally uncommon in carbonatites except for a few occurrences as a secondary mineral
61 (Mackay and Simandl, 2015; and references therein); its presence as a primary mineral is
62 rare (Mariano, 1989). Columbite can be a primary or an alteration product from pyrochlore
63 through an igneous or hydrothermal event (Chakhmouradian et al., 2015; Heinrich, 1966;
64 James and McKie, 1958; Mariano, 1989). James and McKie (1958) were the first to
65 describe the alteration process from pyrochlore to columbite in carbonatite, later named
66 columbitization (Heinrich 1966). Alteration of pyrochlore has been studied recently
67 (Chakhmouradian et al., 2015; Cordeiro et al., 2011; Lumpkin and Ewing, 1995; Nasraoui
68 and Bilal, 2000; Mitchell, 2015; Wall et al., 1996) in lateritic and relatively fresh
69 carbonatites. These works highlight an origin of columbite from the alteration of
70 pyrochlore, although none of the studies showed the conservation of all major elements
71 between pyrochlore and columbite-(Fe), minus the release of Na.

72

73 The economic viability of a Nb exploitation is influenced by the variation in size, shape
74 and chemistry of Nb-bearing minerals as well as by the distribution of different Nb-bearing
75 phases within a deposit. Therefore, a thorough understanding of the mechanisms that
76 control Nb-hosting phases and their alteration are crucial for a comprehension of
77 mineralization associated with carbonatites and potential causes of metallurgy issues, such
78 as the alteration of minerals that can hinder economic exploitation.

79

80 The Saint-Honoré alkaline complex is an ideal setting for the study of carbonatites and
81 their related Nb-hosting minerals as it is currently exploited and accessible to a depth of
82 808 m (2650 feet). Studies regarding mineralization (Fortin-Bélanger, 1977; Thivierge et
83 al., 1983) have been conducted in the weathered upper portion of the carbonatite and more
84 recent studies of the Saint-Honoré carbonatite focused on REE mineralization (Fournier,
85 1993; Grenier et al., 2013; Néron, 2015; Néron et al., 2013) or the origin of ubiquitous
86 halite (Kamenetsky et al., 2015). The main minerals exploited for Nb are
87 fluorcalciopyrochlore (using the pyrochlore classification of Atencio et al. (2010)) and
88 columbite-(Fe). There are four other pyrochlore species (e.g. Sr, Th or U-rich) present in
89 the Saint-Honoré carbonatite (Belzile, 2009; Clow et al., 2011), but they are of minor
90 importance.

91

92 Columbite from the Saint-Honoré carbonatite is part of the iron end-member and hence is
93 classified as columbite-(Fe) (Burke, 2008) (previously named ferrocolumbite). With depth,
94 columbite-(Fe) increases in abundance, becoming a major Nb-bearing mineral. This pattern
95 with depth provides new insights on the genesis of carbonatites, but also presents extractive

96 metallurgy issues for exploitation. In this study, the petrogenesis of pyrochlore and
97 columbite-(Fe) is investigated. The puzzling presence of halite grains observed in minute
98 cavities of weakly altered pyrochlores provides clues about sodium remobilization in
99 carbonatites and the contribution of halite to fenitization.

100

101 *1.1 Geological setting*

102 The Saint-Honoré alkaline complex is located in the Saguenay region, Quebec (Canada).
103 The regional bedrock is the Canadian Shield and is mainly composed of Mesoproterozoic
104 rocks of the Grenville Province (Dimroth et al., 1981; Higgins and van Breemen, 1996).
105 Dimroth et al. (1981) divided the geological province into three units: 1) a gneiss complex
106 that was deformed and migmatized during the Hudsonian Orogeny (1735 Ma); 2)
107 anorthosite and charnockite-magnerite batholiths dating from pre- to post-Grenville
108 orogeny (935 Ma); and 3) calc-alkaline intrusions that cross-cut the host rocks. This late
109 stage, the Iapetan rift system, is related to alkaline activity (Kumarapeli and Saull, 1966)
110 and includes the intrusion of the Saint-Honoré alkaline complex.

111

112 The alkaline complex is composed of a crescent-shaped carbonatite surrounded by alkaline
113 silicate rocks. The host rocks were fenitized by the emplacement of the complex and the
114 fenitization is characterized by sodic-amphiboles, aegirine, sericitized plagioclases as well
115 as green and red carbonate veins (Fortin-Bélanger, 1977). Silicate rocks are represented by
116 three types of syenites: alkaline syenite, nepheline-bearing syenite and syenite foidolites
117 (ijolite-urtite). The presence of xenoliths of altered syenites in the carbonatite suggests

118 silicate rocks are older than the carbonatite. K-Ar dating of the alkaline complex gave an
119 age of 565 Ma (Doig and Barton, 1968). McCausland et al. (2009) report an Ar-Ar age of
120 571 ± 5 Ma from phlogopite and Kamenetsky et al. (2015) report a two-point Rb-Sr model
121 age of 564 ± 8 Ma. More recently, baddeleyite from lamprophyre dikes associated with the
122 Saint-Honoré suite yielded a U-Pb age of 582.1 ± 1.8 Ma (Michael Higgins, UQAC,
123 personal communication, 2015). The carbonatite is covered by Ordovician black shale and
124 limestone.

125

126 The carbonatite complex is generally composed of concentric, subvertical layers of various
127 carbonate types, ranging from calcite in its external portion to dolomite and ankerite toward
128 its core (Fortin-Bélanger, 1977; Thivierge et al., 1983) (Fig. 1). The ankerite facies is
129 known to host an economic REE mineralization (Fournier, 1993; Grenier et al., 2013;
130 Néron et al., 2013). The calcitic outer rim is barren of Nb and REE mineralization and is
131 characterized by the presence of amphiboles. Underground, it is possible to observe several
132 calcite-bearing dikes, lenses of semi-massive to massive magnetite and xenoliths of
133 syenitic rocks throughout the dolomitic facies. Our textural observations, such as hydraulic
134 fracturing and the presence of unaltered calcite grains, suggest the calcitic injections to be
135 from a younger episode of magmatism. The calcitic rocks within the dolomite facies are
136 also younger than the calcitic rocks of the external portion of the carbonatite. This
137 assumption is based on the comparison of accessory minerals, textures and alterations. In
138 other words, the different carbonatitic layers of the Saint-Honoré complex are
139 homogeneous at a regional scale (calcitic, dolomitic and ankeritic carbonates), but are very
140 heterogeneous at the local scale. The complex patterns involving multiple generations of

141 carbonatitic units and alteration fronts suggest a complicated history of multiple injections
142 of differing composition and variable alteration fronts (Fig. 2).

143

144 *1.2 Mining overview*

145 The Saint-Honoré alkaline complex was discovered in 1967 and mining operations began
146 in 1976. Reserves were recently estimated at 416 Mt grading 0.41% Nb₂O₅ (Vallières et
147 al., 2013). Exploitation is currently at a depth of 808 meters (2650 feet) and mineralization
148 is open at depth. Production at the mine accounts for ~8–10% of the global production of
149 Nb₂O₅ (Papp, 2015). Phosphorus (Savard, 1981) and LREE in the Saint-Honoré complex
150 (Grenier et al., 2013; Néron et al., 2013) are also being considered for future exploitation.

151 **2. Methods**

152 *2.1 Sample collection and preparation*

153 Two drill holes at the 1600' level (~490 m) were selected; one facing north and one facing
154 south. These drill holes were selected to cover a wide spectrum of mineralogical
155 assemblages and to allow for study of the dolomitic and calcitic mineralized zones.
156 Furthermore, mineralogy and textures in rocks at this depth are not affected by supergene
157 alteration. During sampling, we ensured that mineralization samples were collected from
158 different facies to best represent the carbonatite. Niobium mineralization in the different
159 Nb-bearing minerals is not evenly distributed in the deposit. The southern portion of the
160 carbonatite is characterized predominantly by pyrochlore mineralization whereas the
161 northern portion contains a higher proportion of columbite-(Fe). The north-facing drill hole
162 length is 235 m and is inclined downwards at 6 °. The length of the south-facing drill hole

163 is 115 m and dips at 31 °. A third drill hole was selected at the 2100-foot level (~640 m) to
164 ensure representability at depth.

165

166 From the cores recovered from the upper two drill holes, 73 polished thin sections were
167 produced. Twenty-three polished thin sections were prepared from the lower drill hole.
168 Nine additional polished thin sections of mineralized lenses from the three drill holes were
169 prepared with a water-free lubricant (acetone) to preserve water-soluble chlorides.

170 *2.2 Sample analysis*

171 We conducted macroscopic observations and selected samples under the supervision of
172 mine geologists. Thin sections were studied at the Université du Québec à Chicoutimi
173 (UQAC) with a Nikon polarizing microscope and cathodoluminescence using a CITL
174 Mk5-1 coupled with a cathodoluminescence stage (Cambridge Image Technology Ltd,
175 Cambridge, UK) and an optical microscope. Most analyses were obtained under the
176 settings of 0.003 mbar, 12 kV and 150 µA. However, voltage and current were often
177 increased to 18 kV and 200 µA, respectively, to observe more discrete colors and zonings.

178

179 A scanning electron microscope (SEM) (JEOL JSM-6480LV) equipped with energy
180 dispersive spectroscopy (EDS) (Oxford x-act) based at UQAC was used to produce back-
181 scattered electron (BSE) images. Analysis parameters were 15 kV and a working distance
182 of 12 mm. The EDS-SEM was used to identify Nb-bearing minerals and undetermined
183 inclusions as well as to confirm the presence of chlorides on thin sections prepared with
184 acetone.

185

186 Major elements were analyzed using a microprobe (JEOL JXA-8900 L) at McGill
187 University (Montréal, Quebec, Canada) having the parameters set at 15 kV, 20 nA and a
188 beam size of 10 μm . Multiple analyses used a beam size of 5 μm to characterize thin zoning
189 and to identify micrometric inclusions within pyrochlore. We applied the ZAF method for
190 matrix corrections.

191

192 Trace elements in pyrochlore and columbite-(Fe) were analyzed by laser ablation
193 inductively coupled plasma mass spectrometry (LA-ICP-MS). Our analyses used an UP-
194 213 laser ablation system (213 nm) from New Wave Research coupled with an Agilent
195 7700x ICP-MS. Calibration was performed by using NIST SRM-610 for pyrochlore with
196 ^{44}Ca as internal standard and GSE-1G for columbite-(Fe) analysis with ^{57}Fe as internal
197 standard. The beam diameter was 100 μm with a pulsing rate of 20 Hz.

198

199 **3. Results**

200 ***3.1 Petrography of the niobium-bearing units***

201 The niobium mineralization is predominantly distributed within the dolomitic portion of
202 the carbonatite although it may also be found in minor amounts within the calcitic facies.

203 There is no significant Nb mineralization in the ferro-carbonatite central core. This study
204 focuses solely on the Nb-bearing units comprising the dolomitic facies and younger
205 mineralized calcitic units enclosed within the dolomitic facies.

206

207 The carbonatite is strongly banded at a centimeter to meter scale (Fig. 2). Mineral
208 proportions are highly variable both between and within the bands. Niobium mineralization
209 appears in the form of elongated subvertical lenses varying from a few millimeters to
210 several meters in width and having a complex geometry. These lenses are also visible
211 within the calcitic units enclosed within the broad dolomitic assemblage. Other petrological
212 units are also observed, including xenoliths of syenites, glimmerites and cumulates of
213 magnetite.

214

215 ***3.1.1 Dolomitic rocks***

216 The dolomitic facies is characterized by the same mineralogical assemblage throughout the
217 complex, composed mainly of medium-grained, hypidiomorphic dolomite free of cleavage
218 with accessory phlogopite, magnetite, pyrite and several types of apatite. Ilmenite,
219 hematite, sphalerite, chlorite, amphibole, quartz, zircon, barite and REE minerals (e.g.
220 bastnäsite and monazite) are also present in trace amounts. Accessory minerals appear
221 disseminated within the carbonatite or concentrated in bands (flowbanding?) forming
222 economic lenses (Fig. 3). The dolomite is generally equigranular and shows no apparent
223 zoning (Fig. 4A). Dolomite does not show any obvious calcitization nor replacement by a
224 secondary mineral. Mineralization is composed of fluorcalciopyrochlore and columbite-
225 (Fe). The dolomitic rocks are usually weakly to moderately altered and are characterized
226 under polarized light by grayish dolomite grains, a light chloritization of phlogopite and a
227 darkening of pyrochlore grains. Rare lamellae of calcite are also observed within some
228 phlogopite grains.

229

230 **3.1.2 Enclosed calcitic units**

231 Enclosed calcitic units are subvertical across the dolomitic units. Hydraulic fracturing of
232 the dolomite rocks near the margins of the calcitic rocks also confirms the interpretation of
233 later calcitic injections (Fig. 4D). They are mineralized and are—from a mineralogical
234 point of view—different from the outer barren calcitic unit of the carbonatite. For example,
235 the outer calcitic unit holds amphiboles and has a green pervasive tint, features not
236 observed in the calcite injections. Unlike the dolomitic rocks, calcitic rocks are medium-
237 to coarse-grained and are idiomorphic with apparent cleavages (Fig. 4B). A mosaic
238 polygonal texture is often visible, but grains are not deformed as is often observed in many
239 other carbonatites (Chakhmouradian et al., 2016). Accessory minerals (Ap, Mag, Phl, Py)
240 are the same as those found in the dolomitic facies, however they are mostly disseminated.
241 The calcitic injections are not altered suggesting they crystallized during or after the
242 alteration event. Furthermore, pyrochlores found in this facies are idiomorphic, often
243 zoned, unaltered and hence light brown. Columbite-(Fe) grains observed in the calcitic
244 injections are heavily fractured and are interpreted as antecrysts from the dolomitic facies.

245

246 **3.2 Nb mineralization**

247 At the 1600' (~485 m) level, the petrography of the mineralization shows that
248 fluorcalciopyrochlore and columbite-(Fe) account for approximately 65% and 35%,
249 respectively, of Nb mineralization. As fluorcalciopyrochlore and columbite-(Fe) are the
250 most abundant and main minerals exploited for Nb at the Saint-Honoré carbonatite, only
251 these two minerals are considered for the remainder of this study.

252

253 ***3.3 Fluorcalciopyrochlore***

254 For our purposes, fluorcalciopyrochlore will be referred to as pyrochlore (Pcl) given that
255 other pyrochlore species are much less abundant and have not been as extensively studied.
256 Fluorcalciopyrochlore (pyrochlore) has been the main mineral exploited for Nb at the
257 Saint-Honoré deposit since 1971. Unaltered pyrochlore grains are usually euhedral,
258 typically 0.01–2 mm in size, but are up to a centimeter in size in a few samples. They are
259 usually light brown to gray with a greenish tint. A few grains are zoned (Fig. 5) and are
260 usually inclusion-free, excepting a few apatite or rare pyrite inclusions. Most of the
261 economic pyrochlore mineralization is associated with magmatic apatite (AP1) in bands,
262 lenses or clusters within the dolomitic unit (Fig. 6). Pyrochlore grains are also distributed
263 randomly in the carbonatitic matrix, but at a much lower proportion. Coarser and zoned
264 pyrochlores are also observed in the calcitic units. The geochemistry of unaltered
265 pyrochlores shows the expected major elements: Ca, Na, Ti and F. In contrast, altered
266 pyrochlores show leaching of most of the Na, F, Ca and Sr as well as the addition of Fe
267 and Mn (Table 1). Fresh, weakly and moderately altered pyrochlores are distinguished by
268 the proportion of pores, their color (from brown to blackish) and their shapes, varying from
269 octahedral to anhedral.

270

271 ***3.4 Columbite-(Fe)***

272 In hand samples, columbite-(Fe) can easily be misidentified as magnetite. It is black with
273 varying shapes and sizes (ranges from 10 μm –1 mm). Under cathodoluminescence,
274 inclusions of calcite and fluorite are easily distinguished by orange and blue colors,
275 respectively (Fig. 5D). The inclusions are irregular in shape and may account for up to 50%

276 of a columbite-(Fe) grain. Calcite and/or fluorite inclusions are a discriminating
277 characteristic of columbite-(Fe). As with pyrochlore, columbite-(Fe) is observed to be
278 disseminated within the dolomitic matrix, but is in a higher proportion within magmatic
279 apatite (AP1). In general, a dark orange microcrystalline apatite (AP2) is associated with
280 columbite-(Fe) (Fig. 6B). AP2 is orange in hand samples, but is dark orange unless under
281 intense light under the microscope. Where columbite-(Fe) is present rather than pyrochlore,
282 darkened dolomite grains and partly chloritized phlogopite are present. A few grains of
283 columbite-(Fe) are observed in the calcitic rocks as xenocrysts with no inclusions of calcite
284 or fluorite. Nevertheless, unlike pyrochlore, columbite-(Fe) grains show no zoning and are
285 generally observed in association with altered dolomite intersected by very fine-grained
286 orange apatite (AP2). Unlike unaltered pyrochlore, columbite-(Fe) has an insignificant
287 content of Ca, Na and F, but a considerable amount of Fe and Mn (Table 2).

288

289 ***3.5 Trace elements in Nb mineralization***

290 To characterize the trace elements in both minerals, LA-ICP-MS analysis was performed
291 on five pyrochlore and five columbite-(Fe) samples (Table 3). Elements including Al, Si,
292 K, Zr, Ta and Hf do not show any significant difference between pyrochlore and columbite-
293 (Fe). These elements, except for K that is undocumented in the pyrochlore crystal structure,
294 are generally found in the B-site and are therefore immobiles (Atencio et al., 2010).
295 Pyrochlore has a very high Th content compared to columbite-(Fe). On the other hand,
296 columbite-(Fe) is enriched in U and it does not follow the same trend as Th as normally
297 expected (both are recognized as being held in the A-site). Transitional metals such as V

298 are surprisingly high in columbite-(Fe), up to 100× higher than in the pyrochlore samples
299 (Fig. 7).

300

301 REEs also display large variations in abundance between pyrochlore and columbite-(Fe)
302 samples. LREE abundance in pyrochlore is nearly ten times greater than in columbite-(Fe)
303 whereas HREE and Y abundance is significantly higher in the columbite-(Fe) (Table 3,
304 Fig. 7 & 8). A comparison of the median content of REEs in pyrochlore from the Aley
305 carbonatite (Chakhmouradian et al., 2015) and pyrochlore from the Saint-Honoré
306 carbonatite shows the latter to have lower or similar REE amounts. Major elements (e.g.
307 Na, Ca, F) are, however, found at higher amounts in pyrochlores from Saint-Honoré than
308 found in the Aley carbonatite.

309

310 *3.6 Crystallization of halite*

311 Sodium is a major cation in fluorcalciopyrochlore at the Saint-Honoré carbonatite. While
312 Ca and F are both observed as inclusions of calcite and fluorine within columbite-(Fe), Na-
313 bearing minerals are not observed as inclusions. However, halite is ubiquitous in the Saint-
314 Honoré carbonatite (Guillaume Matton, Niobec Inc., personal communication, 2015) and
315 is either observed disseminated or filling fractures. Its proportion is difficult to estimate
316 underground as it is leached during mine operations, such as drilling and logging. Halite
317 was always observed in pores of moderately altered pyrochlore (Fig. 9A & B) in those
318 samples with a decreased Na content. Kamenetsky et al. (2015) described halite crystals in
319 pyrochlore melt inclusions (a conclusion that relies heavily on interpretation), but we could
320 not find any halite in fresh pyrochlore nor within columbite-(Fe) grains.

321

322 **4. Discussion**

323 The study of the mineralization highlighted a strong association of pyrochlore and
324 columbite-(Fe) with the accessory minerals. An intrinsic relationship between pyrochlore
325 and columbite-(Fe) was also identified by the presence of calcite and fluorite inclusions
326 under cathodoluminescence and, under SEM analysis, grains showing ongoing alteration
327 from pyrochlore into columbite-(Fe). Alteration appears to be hydrothermal and the
328 enrichment of Cl in columbite-(Fe) reinforces this interpretation. Chloride, along with
329 leached Na from pyrochlore, could be involved in the formation of halite.

330 ***4.1 Petrology of the Nb-bearing units and mineralization***

331 Within the dolomitic units, apatite and other accessory minerals (Phl, Mag, Py) are
332 agglomerated in lenses. Considering the post-Grenvillian geological setting, this foliation-
333 like pattern is interpreted as an igneous texture (flowbanding) induced by the low viscosity
334 of the carbonatitic magma (Treiman, 1989). Alternatively, accessory minerals in the
335 calcitic units are generally disseminated and lenses are less frequent. It suggests that the
336 magma chamber was less turbulent in the late magmatic stage. These calcitic units are
337 thought to be derived from a later event given their coarser grain size, the presence of well-
338 developed cleavages and the absence of alteration. Pyrochlores in these calcitic units are
339 euhedral and mostly unaltered. A few columbite-(Fe) grains are also visible, but they are
340 highly fractured without calcite and fluorite inclusions. These columbite-(Fe) grains are
341 likely antecrysts from the dolomitic facies. Antecrysts refer to crystals that did not
342 crystallize from the calcitic magma, but still have a relationship with the magma (as
343 described in Charlier et al., 2005).

344

345 Both columbite-(Fe) and fluorcalciopyrochlore are intimately associated with apatite, a
346 common characteristic in carbonatites (Hogarth et al., 2000; Knudsen, 1989). The first type
347 of apatite (AP1) is translucent, euhedral and zoned as described by Chakhmouradian et al.
348 (2017). Primary textures suggest this apatite to be of magmatic origin. A few inclusions of
349 AP1 were observed within pyrochlore grains suggesting it is syngenetic. AP1 and
350 pyrochlore might have crystallized earlier in the magmatic evolution as Nb was probably
351 transported with phosphate and fluorine complexes resulting in the co-precipitation of
352 apatite and fluorcalciopyrochlore (Hogarth et al., 2000; Knudsen, 1989). As proposed by
353 Jago and Gittins (1991), fluorine might lower melting temperatures, thereby precipitating
354 pyrochlore. To have pyrochlore crystallized instead of other Nb-bearing minerals, the
355 liquid must have more than 1% F (Mitchell and Kjarsgaard, 2004). Magmatic apatites
356 (AP1) appear to be in equilibrium with the second type of apatite (AP2, fine-grained,
357 anhedral and orange) as they are unmodified when cross-cut by AP2. However, AP1
358 produces a thin outer white rim under cathodoluminescence (Fig. 6D). The AP2 follows
359 random patterns in the carbonatite. Most of the pyrochlores are altered by the AP2:
360 pyrochlore darkens, develops pores and tips are truncated.

361

362 *4.2 Alteration of pyrochlore*

363 Although some replacement of pyrochlore by columbite-(Fe) from Saint-Honoré has been
364 documented (Mitchell, 2015), a lack of proper samples has previously hindered a complete
365 interpretation. Our study provides more complete evidence for the removal of A-site

366 cations and the transitional sequence of alteration of fluorcalciopyrochlore to columbite-
367 (Fe).

368

369 According to the published literature (e.g. Lumpkin and Ewing, 1995), the first stage of the
370 alteration of pyrochlore is the leaching of Na. When Na is completely leached, minor Fe
371 and Mn begin filling vacancies in the A-site. At the same time, F is slowly leached from
372 the Y-site and Cl is suspected to replace F. Alteration then leaches Ca and Sr with Fe and
373 Mn partly filling this vacancy leading to crystals having a composition of $(\text{Fe,Mn})\text{Nb}_2\text{O}_6$,
374 referred to as columbite. Moreover, if alteration persists, tiny pores, as small as 1 μm , may
375 be left. The smallest pores are orientated (Fig. 10A) and are related to zoning, crystal
376 structure weaknesses or fractures. The larger pores containing halite, calcite and fluorite
377 are irregular in shape, angular and never spherical (Fig. 9A & B) as it would be expected
378 for melt inclusions. Inclusions of altered pyrochlore to columbite-(Fe) are also visible (Fig.
379 10A).

380

381 The alteration of pyrochlore correlates with the alteration level of the carbonates and other
382 accessory minerals, such as phlogopite to chlorite. Thus, alteration of pyrochlore depends
383 on its physical properties (fractures or any other crystal weaknesses) and corrosion along
384 the alteration front. For the Saint-Honoré samples, microprobe (Fig. 10A, C & D) and BSE
385 imagery (Fig. 10B) clearly show the columbitization process along margins and fractures.
386 Pyrochlore is altered stepwise into columbite-(Fe) as the fluid weakens the structure
387 through leaching of the major cations. Pyrochlore is clearly not in equilibrium with the

388 fluid; a pyrochlore in contact with a fully altered pyrochlore to columbite-(Fe) will tend to
389 transform as well (Fig. 10).

390

391 In addition to the leaching of Na, Ca and Sr and their replacement by Fe and Mn on the A-
392 site, other trace element levels are modified during alteration. Our microprobe and LA-
393 ICP-MS analyses showed an enrichment of Cl, transition metals (Cr, V, Y) and HREEs as
394 well as a decrease in LREEs in columbite-(Fe) relative to pyrochlore (Fig. 7 & 8). A loss
395 in LREEs in columbite-(Fe) might be due to lower compatibility of LREEs than HREEs in
396 common rock-forming minerals (Linnen et al., 2014) and are therefore leached out during
397 alteration. These LREEs are found as fine needles of bastnäsite in immediate vicinity of
398 weakly altered pyrochlore. Columbite-(Fe) had an average of 510 ± 155 ppm Cl (Table 2)
399 whereas pyrochlores had Cl concentrations below detection limit (70 ± 160 ppm Cl; Table
400 1). A Cl enrichment during alteration (Fig. 11) is therefore evident and a Cl-rich fluid
401 suggests hydrothermal activity. Weathering can be dismissed as we observed no
402 petrographic evidence, such as gypsum or karst, at the sampled levels. Geodes, karsts and
403 highly altered carbonates are observed in the upper 120 m of the Saint-Honoré carbonatite
404 (Thivierge et al., 1983), but not any deeper. Thus, supergene alteration (weathering) as the
405 source of Cl is less likely. Unfortunately, Cl in pyrochlore is poorly documented and its
406 position in the crystal structure remains unclear. However, based on its chemical
407 similarities with F, it is assumed to be replacing F in the Y-site.

408

409 In pyrochlore, the mean value of Y_2O_3 is below detection limit (850 ± 761 ppm) while its
410 content in columbite-(Fe) exceeds 3920 ± 754 ppm. Yttrium behaves similarly to other

411 HREEs and is therefore considered as a heavy rare earth element sensu lato. It replaces A-
412 site cations (Atencio et al., 2010). A HREE enrichment of a magnitude of ~5 is observed
413 in columbite-(Fe) (Table 3; Fig. 7). This is similar to results from the Aley carbonatite
414 where pyrochlore and fersmite were compared (Chakhmouradian et al., 2015). This also
415 agrees with the results of Néron (2013, unpublished data) who observed a HREE-rich rim
416 around apatite and suggested a hydrothermal event for the REE mineralization in the Fe-
417 carbonatite of the Saint-Honoré complex. No other primary mineral in the carbonatite has
418 shown a considerable Y content. This suggests that Y and HREE did not originate from an
419 earlier magmatic stage but from a later event.

420

421 The enrichments of Y, HREEs or any other metals could arguably have been related to a
422 volume change due to columbite-(Fe) collapsing during alteration. A gain of roughly 10%
423 Nb₂O₅ is observed in columbite-(Fe) compared to unaltered pyrochlore. On the other hand,
424 heavy REEs (including Y) increase 4 to 6× in columbite-(Fe). Considering Nb is immobile
425 and varies much less than any other enriched element, this hypothesis of an enrichment by
426 a volume change is unlikely.

427

428 An intriguing transitional alteration state was also observed. The mineral is called
429 “ferropyrochlore” by the mine geologists, although it does not fit the classification of
430 Atencio et al. (2010). Geochemically, this pyrochlore has completely lost its Na, but only
431 half of its Ca. As Ca is leached, it is replaced by Fe±Mn. Analyses have shown a pyrochlore
432 with 7% of FeO and 7% CaO. The sum of major divalent oxides (FeO+MnO+CaO+SrO)
433 during alteration is stable at approximately 17% and increases above 21% when Ca is

434 completely leached out and the alteration to columbite-(Fe) is complete. Fersmite is known
435 as a transitional state of alteration of pyrochlore to columbite-(Fe) or as an alteration
436 product of columbite-(Fe) (Lumpkin and Ewing, 1995). However, fersmite is not observed
437 anywhere in the carbonatite.

438

439 ***4.3 Origin of alteration***

440 Based on Lumpkin and Ewing (1995), the ternary diagram of A-site monovalent and
441 divalent cations and vacancies can be used to define the origin of the alteration. Alteration
442 can be either a late magmatic alteration, a hydrothermal event or a supergene alteration
443 (Nasraoui and Bilal, 2000; Zurevinski and Mitchell, 2004). At the Saint-Honoré
444 carbonatite, the use of the ternary diagram is fairly straight-forward considering: (1) there
445 are only two major A-site cations in the pyrochlore, which are respectively monovalent and
446 divalent (Na and Ca); (2) various samples show various stages of alteration of pyrochlore;
447 and (3) more than 800 microprobe analyses were used. This includes 543 microprobe
448 analyses from 1978 (SOQUEM) and 136 from 2011 (SGS Canada). To ensure
449 reproducibility, we added 145 new microprobe analyses performed on pyrochlore and
450 columbite-(Fe).

451

452 Apfu (atoms per formula unit) of the A-site were calculated with a structural formula based
453 on the assumption that B-site anions are immobile and therefore have a sum of two. Results
454 were plotted into the triangular (A-site monovalent and divalent cations and vacancy) plot
455 to provide an alteration trend (Fig. 12). Fe and Mn introduced during alteration were
456 calculated as A-site cations to evaluate more precisely the vacancy in the A-site. Otherwise,

457 fully transformed pyrochlore to columbite-(Fe) would have plotted in the upper part of the
458 vacancy field implying an origin by supergene alteration, although our observations clearly
459 show that this is not the case for the Saint-Honoré complex. This is a false assumption
460 considering that Fe and Mn are divalent cations (as are Ca and Sr) and are therefore
461 required in the calculations. Moreover, this method was developed solely for pyrochlore
462 and not for columbite-(Fe). However, plotting columbite-(Fe) with pyrochlore fits the
463 purpose in the diagram as it reinforces the alteration trend. Figure 12 clearly shows a
464 transitional trend from a primary pyrochlore to a hydrothermally-altered pyrochlore into
465 columbite-(Fe). This is in accordance with the higher Cl content of columbite-(Fe) and the
466 HREE rim around AP1.

467

468 The hypothesis that the alteration is of a hydrothermal origin is strengthened by the
469 enrichment of Cl and HREEs in columbite-(Fe) (Tables 1 & 2). Chloride suggests an
470 aqueous fluid whereas the presence of HREE follows a similar description of hydrothermal
471 enrichment in the ferro-carbonate core of the carbonatite (Néron, 2015). However, the
472 presence of fluorite suggests that F was probably a component of the hydrothermal fluid.

473

474 ***4.4 Origin of halite***

475 The presence of ubiquitous halite in the Saint-Honoré carbonatite is intriguing. Sodium is
476 certainly magmatic in the Saint-Honoré carbonatite as it is a major constituent of
477 fluorcalciopyrochlore (up to 8% Na₂O), one of the first minerals with apatite to crystallize
478 in a carbonatitic magma (Hogarth et al., 2000; Knudsen, 1989; Hogarth et al., 2000). The

479 strong relationship of pyrochlore to apatite and the textural evidence also argue for a
480 magmatic origin.

481

482 The origin of chlorine is, however, enigmatic. From the spatial distribution of halite in and
483 around magmatic minerals from the Saint-Honoré carbonatite, Kamenetsky et al. (2015)
484 proposed halite, and specifically chlorine, to be mantle-derived, based on the presence of
485 halite in melt inclusions found in pyrochlore, apatite, phlogopite and pyrite. Although we
486 did not study phlogopite, apatite and pyrite, our study of the Nb-bearing minerals of the
487 carbonatite offers a slightly different understanding of the petrogenesis of halite.
488 Petrographic observations and geochemical analyses of pyrochlore and columbite-(Fe)
489 demonstrate that Na was leached during alteration whereas Cl was related to hydrothermal
490 fluid. Thus, the Na is considered to be magmatic in origin and some Cl as hydrothermal
491 (Tremblay et al., accepted). Although it is possible that some halite in the carbonatite is
492 indeed magmatic, given the observation of halite in pyrochlore, halite crystals were all
493 produced by the release of Na during the alteration of pyrochlore. Interestingly, the only
494 units showing halite are those having more radiogenic Sr (Kamenetsky et al., 2015). As
495 such, these observations confirm that Na has a magmatic origin, but that some of the Cl is
496 fluid-related. A portion of the halite has therefore a magmato-hydrothermal origin. The
497 absence of Cl in other magmatic minerals (e.g. apatite and phlogopite) reinforces the
498 hypothesis of Cl being from a hydrothermal fluid and not from a primary origin. It does
499 not preclude that some halite might have crystallized from a magmatic event, but none of
500 our observations can confirm this hypothesis.

501

502 A mass balance study determined whether the alteration of pyrochlore was an important
503 source of Na for post-magmatic activity such as fenitization. We based our calculations on
504 the Na content of 51,600 whole rock analyses. It is important to specify that these results
505 come from various rock types of the mine property, including units having little halite.
506 Values follow a log-normal distribution and range from below the detection limit to 5.77%
507 with a log-normal mean of 0.329%. Cl is a readily soluble element and is quite likely lost
508 during drilling, mine operations, sample preparation, etc. Thus, results from whole rock
509 analysis are considered to be less reliable. Therefore, we used the Cl content from an
510 unpublished environmental study of mine effluents, as we consider that it offers a better
511 overall sampling of Cl content for the complete carbonatite complex. However imperfect,
512 it offers quantitative limits to the model. Analyses of 119 samples produced a Cl content
513 of 0.008 to 1.88% and an arithmetic mean value of 0.429%, with a standard deviation of
514 0.337%. As the Cl/Na ratio is 1.54 in halite, and $0.429\%/1.54 < 0.329\%$, then it is apparent
515 that Na is the limiting factor. Since there are no other major Na-bearing minerals in the
516 carbonatite other than pyrochlore and halite, a maximum proportion of 0.622% halite could
517 be formed if all Na was used. Other chlorides were also observed, however only in
518 anecdotal proportions; a few grains of sylvite (KCl), hydrophilite (CaCl₂) and
519 chloromagnesite (MgCl₂) were identified by SEM. It is possible they may have
520 recrystallized during the preparation of the thin sections.

521

522 To quantify the amount of Na leached during the alteration of pyrochlore, the amount of
523 pyrochlore in the carbonatite must be constrained. Historic whole rock analysis shows a
524 mean Nb₂O₅ of 0.427% throughout the carbonatite, including holes drilled in barren units.

525 Considering fluorcalciopyrochlore accounted for more than 95% of the Nb-bearing
526 minerals (Nb-rutile and other minor phases account for less than 5%) before alteration, we
527 calculate a disseminated 0.615% pyrochlore in the carbonatite. This is based on pyrochlore
528 containing approximately 66% Nb₂O₅. Hence, 0.615% pyrochlore at 5.42% Na (mean
529 value of microprobe analysis) gives a weight percentage of 3.33% Na. Therefore, if all
530 pyrochlore is indeed altered into columbite-(Fe), this limits the quantity of halite at 0.085%.

531

532 Based on the logarithmic mean content of Na (as Na has a log-normal distribution) in the
533 carbonatite and the possible output of Na during alteration, pyrochlore alteration might
534 contribute up to 10% of the necessary Na to form halite. Our results show that it is unlikely
535 the Na needed to crystallize halite comes entirely from the alteration of pyrochlore; it was
536 demonstrated, however, that it does contribute to some degree. The remaining Na needed
537 to form the halite is thought to come from a Na-rich late magmatic event that was affected
538 by hydrothermal activity, solubilizing Na and forming halite as soon as the parameters had
539 changed. Furthermore, current resource estimates at the mine suggest that the proportion
540 of pyrochlore increases with depth. If confirmed, the presence of Na would be higher and
541 hence contributing even more to the mass balance. At even greater depths, it is possible
542 that with the increased proportion of pyrochlore, Na from these pyrochlore units could have
543 been released during hydrothermalism and, because Na is easily soluble, it could have been
544 transported upwards in the carbonatite to form halite. This would reinforce the
545 interpretation that the alteration of pyrochlore is a major contributor of Na.

546

547 **5. Conclusion**

548 The Saint-Honoré carbonatite offers a significant opportunity to study carbonatites:
549 sampling is available down to ~640 m deep and samples are devoid of weathering below
550 ~120 m. Samples are also easily accessible and very abundant. The petrological study of
551 the main Nb-bearing minerals, fluorcalciopyrochlore and columbite-(Fe), shed light on
552 their genesis and the alteration process. Grains of varying alteration levels showed
553 transitional states of alteration beginning at the crystal margins or within fractures. Na, Ca
554 and F are gradually leached out, creating a vacancy as the crystal structure changes. During
555 this process, inclusions of calcite and fluorite are formed within columbite-(Fe). A few
556 weakly altered pyrochlores had preserved halite in their pores. The Cl, Y and HREE
557 enrichments in columbite-(Fe) and the leaching of LREEs suggest this is a possible source
558 of crystallization of halite and a HREE-bearing, water-rich fluid. This refines the
559 interpretation of Kamenetsky et al. (2015): not all halite is magmatic, as some has a
560 hydrothermal origin.

561

562 Considering that most carbonatites are studied from outcrop samples or through shallow
563 drilling where weathering is prevalent, this study provides much needed insight into the
564 deeper evolution of carbonatites. We also provided new information regarding the
565 columbitization process and its contribution in the formation of halite in the Saint-Honoré
566 carbonatite. Chloride could have played an important role in the transport of REEs in
567 ankeritic rocks. The presence of Cl along with HREEs within columbite-(Fe) suggest that
568 the chlorine complex is an excellent carrier for REE as proposed by Migdisov and
569 Williams-Jones (2014).

570

571 **Acknowledgements**

572 This work was supported by a Natural Sciences and Engineering Research Council of
573 Canada grant to L. Paul Bédard. The UQAC Foundation and DIVEX are thanked for
574 scholarship funds to first author. Our discussions about the deposit with Alexis Gauthier-
575 Ross and Louis-Mathieu Tremblay of Niobec Inc. were greatly appreciated. Vadim
576 Kamenetsky is thanked for sharing his additional data and pictures of the halite from Saint-
577 Honoré. The reviewers are thanked for their help in improving the manuscript. The
578 manuscript had its English improved by Murray Hay (Maxafeau Editing Services).

579 **References**

- 580 Atencio, D., Andrade, M.B., Christy, A.G., Gieré, R., and Kartashov, P.M., 2010. The
581 pyrochlore supergroup of minerals: Nomenclature. *The Canadian Mineralogist*, 48, 673–
582 698.
- 583 Belzile, E., 2009. NI 43-101 Technical report for Niobec Mine, Quebec, Canada,
584 February 2009. IAMGOLD Corporation, 104p.
- 585 Burke, E.A.J., 2008. Tidying up mineral names: An IMA-CNMNC scheme for suffixes,
586 hyphens and diacritical marks. *The Mineralogical Record*, 39, 131–135.
- 587 Cerný, P., 1989. Characteristics of pegmatite deposits of tantalum. In: Möller, P., Cerný,
588 P., and Saupé, F. (eds.) *Lanthanides, Tantalum and Niobium*. Springer-Verlag, Berlin-
589 Heidelberg, 195–239.
- 590 Chakhmouradian, A.R., Reguir, E.P., Zaitsev, A.N., Couëslan, C., Xu, Cheng, Kynický,
591 J., Mumin, A.H., and Yang, P., 2017. Apatite in carbonatitic rocks: Compositional
592 variation, zoning, element partitioning and petrogenetic significance. *Lithos*, 274–275,
593 188–213.
- 594 Chakhmouradian, A.R., Reguir, E.P., and Zaitsev, A.N., 2016. Calcite and dolomite in
595 intrusive carbonatites. I. Textural variations. *Mineralogy and Petrology*, 110, 333–360.
- 596 Chakhmouradian, A.R., Reguir, E.P., Kressall, R.D., Crozier, J., Pisiak, L.K., Sidhu, R.,
597 and Yang, P., 2015. Carbonatite-hosted niobium deposit at Aley, northern British
598 Columbia (Canada): Mineralogy, geochemistry and petrogenesis. *Ore Geology Reviews*,

599 64, 642–666.

600 Chakmouradian, A.R., and Wall, F., 2012. Rare earth elements: minerals, mines,
601 magnets (and more). *Elements*, 8, 333–340.

602 Charlier, B.L.A., Wilson, C.J.N., Lowenstern, J.B., Blake, S., Van Calsteren, P.W., and
603 Davidson, J.P., 2005. Magma generation at a large, hyperactive silicic volcano (Taupo,
604 New Zealand) revealed by U-Th and U-Pb systematics in zircons. *Journal of Petrology*,
605 46, 3–32.

606 Clow, G.G., Salmon, B., Lavigne, M., McDonough, B., Pelletier, P., and Vallières, D.,
607 2011. NI 43-101 Technical report on expansion options at the Niobec mine, Québec,
608 Canada. IAMGOLD Corporation, 204p.

609 Cordeiro, P.F.O., Brod, J.A., Palmieri, M., Oliveira, C.D., Barbosa, E.S.R., Santos, R.V.,
610 Gaspar, J.C., and Assis, L.C., 2011. The Catalão I niobium deposit, central Brazil:
611 Resources, geology and pyrochlore chemistry. *Ore Geology Reviews*, 41, 112–121.

612 Decrée, S., Boulvais, P., Tack, L., André, L., and Baele, J.-M., 2015. Fluorapatite in
613 carbonatite-related phosphate deposits: the case of the Matongo carbonatite (Burundi).
614 *Mineralium Deposita*, 51, 453–466.

615 Dimroth, E., Woussen, G., and Roy, D.W., 1981. Geologic history of the Saguenay
616 Region, Quebec (Central Granulite Terrain of the Grenville Province): a working
617 hypothesis. *Canadian Journal of Earth Sciences*, 18, 1506–1522.

618 Doig, R., and Barton, J.M., 1968. Ages of carbonatites and other alkaline rock in Québec.

619 Canadian Journal of Earth Sciences, 7, 22–28.

620 Fortin-Bélanger, M., 1977. Le complexe annulaire à carbonatites de St-Honoré (P.Q.
621 Canada) et sa minéralisation à niobium : étude pétrographique et géochimique. M.Sc.
622 thesis, Université du Québec à Chicoutimi, Chicoutimi, Canada, 210p.

623 Fournier, A., 1993. Magmatic and hydrothermal controls of LREE mineralization of the
624 St-Honoré Carbonatite, Québec. Unpublished M.Sc. thesis, McGill University, Montréal,
625 Canada, 95p.

626 Giebel, R.J., Gauert, C.D.K., Marks, M.A.W., Costin, G., and Markl, G., 2017. Multi-
627 stage formation of REE minerals in the Palabora carbonatite complex, South Africa.
628 American Mineralogist, 102, 1218–1233.

629 Grenier, L., Tremblay, J.F., and Sirois, R., 2013. NI 43-101 Technical report, updated
630 mineral resource estimate for rare earth elements, 2012. IAMGOLD Corporation, 166p.
631 <http://www.infomine.com/index/pr/PB/39/93/PB399305.PDF>. Accessed 13 March 2017.

632 Heinrich, E.W., 1970. The Palabora carbonatitic complex; a unique copper deposit. The
633 Canadian Mineralogist, 10, 585–598.

634 Heinrich, E.W., 1966. The geology of carbonatites. Rand McNally, Chicago. 555p.

635 Higgins, M.D., and van Breemen, O., 1996. Three generations of anorthosite-mangerite-
636 charnockite-granite (AMCG) magmatism, contact metamorphism and tectonism in the
637 Saguenay-Lac-Saint-Jean region of the Grenville Province, Canada. Precambrian
638 Research, 79, 327–346.

639 Hogarth, D.D., Williams, C.T., and Jones, P., 2000. Fresh rock zoning in pyrochlore
640 group minerals from carbonatites. *Mineralogical Magazine*, 64, 683–697.

641 Hogarth, D.D., 1977. Classification and nomenclature of the pyrochlore group. *American*
642 *Mineralogist*, 62, 403–410.

643 James, T.C., and McKie, D., 1958. The alteration of pyrochlore to columbite in
644 carbonatites in Tanganyika. *Journal of the Mineralogical Society*, 31, 889–902.

645 Jago, B.B., and Gittins, J., 1991. The role of fluorine in carbonatite magma evolution.
646 *Nature*, 349, 56–58.

647 Kamenetsky, V.S., Mitchell, R.H., Maas, R., Giuliani, A., Gaboury, D., and Zhitova, L.,
648 2015. Chlorine in mantle-derived carbonatite melts revealed by halite in the St.-Honoré
649 intrusion (Québec, Canada). *Geology*, 43, 687–690.

650 Knudsen, C., 1989. Pyrochlore group minerals from the Qaqarssuk carbonatite complex.
651 In: Möller, P., Cerný, P., and Saupé, F. (eds.) *Lanthanides, Tantalum and Niobium*.
652 Springer-Verlag, Berlin-Heidelberg, 80–99.

653 Kumarapeli, P.S., and Saull, V.A., 1966. The St. Lawrence valley system: A North
654 American equivalent of the East African rift valley system. *Canadian Journal of Earth*
655 *Sciences*, 3, 639–658.

656 Le Bas, M.J., 1981. Carbonatite magmas. *Mineralogical Magazine*, 44, 133–140.

657 Linnen, R.L., Samson, I.M., Williams-Jones, A.E., and Chakhmouradian, A.R., 2014.

658 Geochemistry of the rare-earth element, Nb, Ta, Hf, and Zr deposits. In: Holland, H.D.,
659 and Turekian, K.K. (eds.) *Treatise on Geochemistry*, Second Edition, Oxford: Elsevier,
660 13, 543–568.

661 Lumpkin, G.R., 1998. Composition and structural state of columbite – tantalite from the
662 Harding Pegmatite, Taos County, New Mexico. *The Canadian Mineralogist*, 36, 585–
663 599.

664 Lumpkin, G.R., and Ewing, R.C., 1995. Geochemical alteration of pyrochlore group
665 minerals: Pyrochlore subgroup. *American Mineralogist*, 80, 732–743.

666 Mackay, D.A.R., and Simandl, G.J., 2015. Pyrochlore and columbite-tantalite as indicator
667 minerals for specialty metal deposits. *Geochemistry: Exploration, Environment, Analysis*,
668 15, 167–178.

669 Mackay, D.A.R., and Simandl, G.J., 2014. Geology, market and supply chain of niobium
670 and tantalum – a review. *Mineralium Deposita*, 49, 1025–1047.

671 Mariano, A.N., 1989. Nature of economic mineralization in carbonatites and related
672 rocks. In: Bell, K. (ed.) *Carbonatites: genesis and evolution*. Unwin Hyman, London,
673 149–176.

674 McCausland, P.J., Pisarevsky, S., Jourdan, F., and Higgins, M., 2009. Laurentia at 571
675 Ma: Preliminary paleomagnetism and Ar-Ar age of the Ediacaran St Honore alkali
676 intrusion, Quebec. *Proceedings, American Geophysical Union–Geological Association of*
677 *Canada–Mineralogical Association of Canada–Canadian Geophysical Union, Joint*

678 Assembly, Toronto, Abstract GA12A-01.

679 Migdisov, A., and Williams-Jones, A.E., 2014. Hydrothermal transport and deposition of
680 the rare earth elements by fluorine-bearing aqueous liquids. *Mineralium Deposita*, 49,
681 987–997.

682 Mitchell, R.H., 2015. Primary and secondary niobium mineral deposits associated with
683 carbonatites. *Ore Geology Reviews*, 64, 626–641.

684 Mitchell, R.H., Kjarsgaard, B.A., 2004. Solubility of niobium in the system $\text{CaCO}_3\text{-CaF}_2\text{-}$
685 NaNbO_3 at 0.1 GPa pressure: implications for the crystallization of pyrochlore from
686 carbonatite magma. *Contributions to Mineralogy and Petrology*, 148, 281–287.

687 Mulja, T., Williams-Jones, A.E., Martin, R.F., and Wood, S.A., 1996. Compositional
688 variation and structural state of columbite-tantalite in rare-element granitic pegmatites of
689 the Preissac-Lacorne batholith, Quebec, Canada. *American Mineralogist*, 81, 146–157.

690 Nasraoui, M., and Bilal, E., 2000. Pyrochlores from the Lueshe carbonatite complex
691 (Democratic Republic of Congo): a geochemical record of different alteration stages.
692 *Journal of Asian Earth Sciences*, 18, 237–251.

693 Néron, A., 2015. Caractérisation de la minéralisation de la zone à terres rares de la
694 carbonatite de Saint-Honoré, Québec, Canada. M.Sc. thesis, Université du Québec à
695 Chicoutimi, Québec, Canada, 70p.

696 Néron, A., Bédard, L.P., Gaboury, D., and Thivierge, S., 2013. Preliminary
697 characterization of the REE mineralization of the St-Honoré ferro-carbonatite (Québec,

698 Canada). Mineral deposit research for a high-tech world: 12th Society for Geology
699 Applied to Mineral Deposits (SGA) biennial meeting in Uppsala (Sweden), Program with
700 Abstracts.

701 Papp, J.F., 2015. Niobium (Columbium). In: United States Geological Survey, Mineral
702 Commodity Summaries 2015, 110–111.

703 Roskill, 2017. Niobium: Market outlook to 2017, 12th edition.
704 <https://roskill.com/product/niobium-market-outlook-2017/>. Accessed March 13, 2017.

705 Savard, J.Y., 1981. Étude de mise en valeur des rejets de carbonate-apatite de la mine
706 Niobec dans le but d'une utilisation comme engrais en agriculture. M.Sc. thesis,
707 Université du Québec à Chicoutimi, Québec, Canada, 147p.

708 Thivierge, S., Roy, D.-W., Chown, E.H., and Gauthier, A., 1983. Évolution du complexe
709 alcalin de St.-Honoré (Québec) après sa mise en place. *Mineralium Deposita*, 18, 267–
710 283.

711 Treiman, A.H., 1989. Carbonatite magma: properties and processes. In: Bell, K. (ed.)
712 *Carbonatites: genesis and evolution*. Unwin Hyman, 89–104.

713 Tremblay, J., Bédard, L.P., Matton, G., Accepted. Halite at the Saint-Honoré carbonatite:
714 an insight into a magmatohydrothermal process. Society for Geology Applied to Mineral
715 Deposits, 14th Biennial meeting, Quebec City, August 20–23, 2017.

716 Vallières, D., Ferlatte, G., Sirois, R., Tremblay, J.-F., Pelletier, P., and Gaultier, P., 2013.
717 NI 43-101 Technical Report, Update on Niobec Expansion, December 2013. 305p.

718 Wall, F., Williams, C.T., and Woolley, A.R., 1996. Pyrochlore from weathered
719 carbonatite at Lueshe, Zaire. *Mineralogical Magazine*, 60, 731–750.

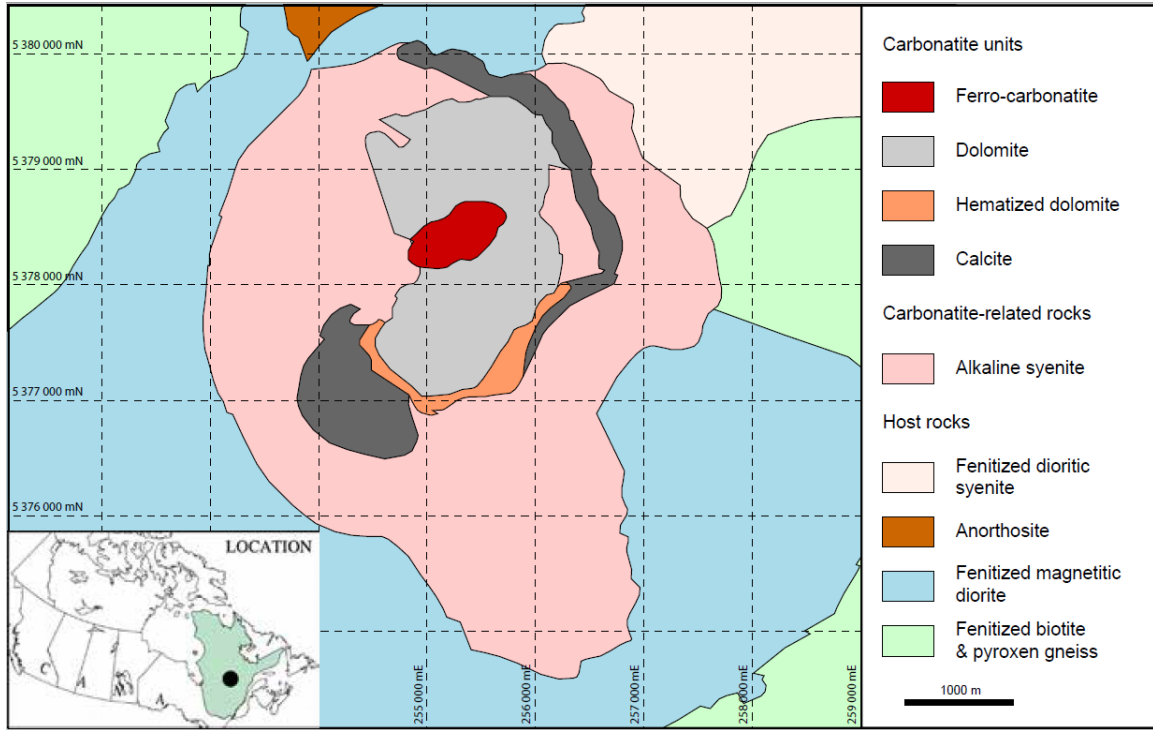
720 Wall, F., Williams, C.T., Woolley, A.R., 1999. Pyrochlore in niobium ore deposits. In:
721 Stanley, C.J. (ed.) *Mineral deposits: processes to processing*. Balkema Publishers,
722 Rotterdam 1, 687–690.

723 Wyllie, P.J., 1966. Experimental studies of carbonatite problems: the origin and
724 differentiation of carbonatite magmas. In: Tuttle, O.F., and Gittins, J. (eds.) *Carbonatites*.
725 Interscience Publishers, New York, 311–352.

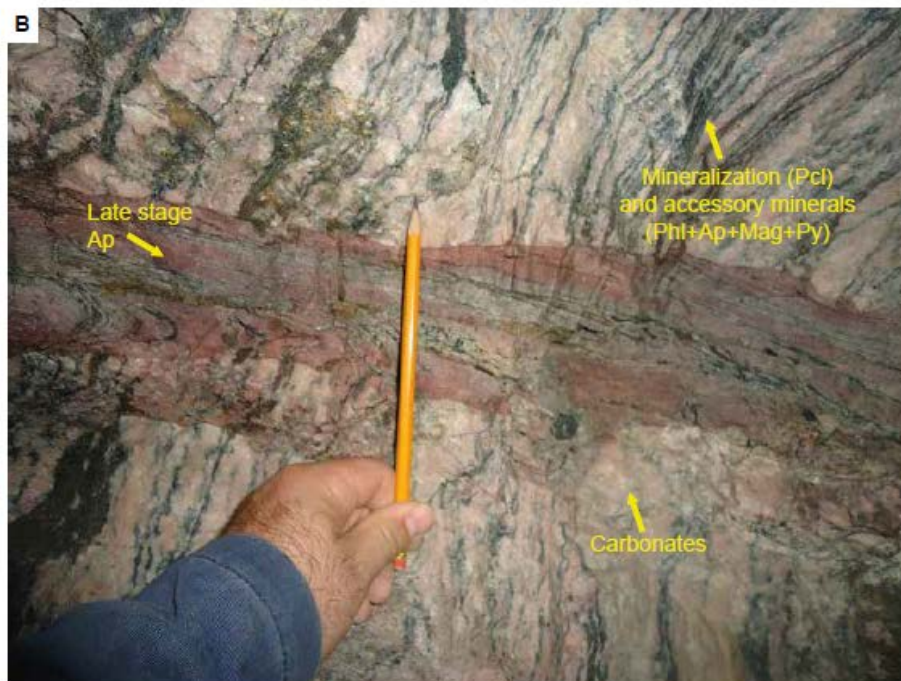
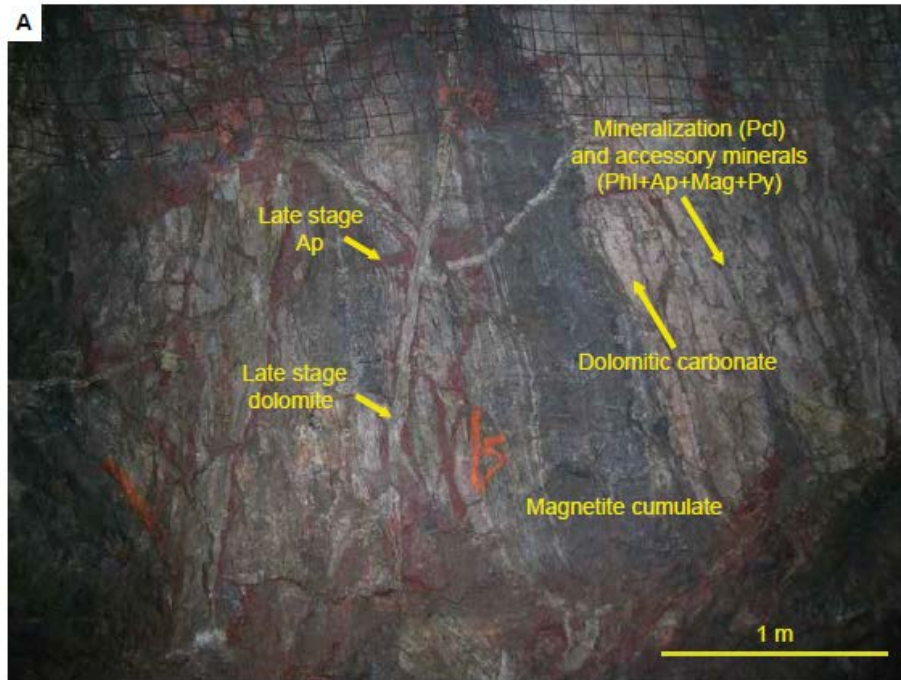
726 Zurevinski, S.E., and Mitchell, R.H., 2004. Extreme compositional variation of
727 pyrochlore-group minerals at the Oka carbonatite complex, Quebec: Evidence of magma
728 mixing? *The Canadian Mineralogist*, 42, 1159–1168.

729

730 **Figure captions**



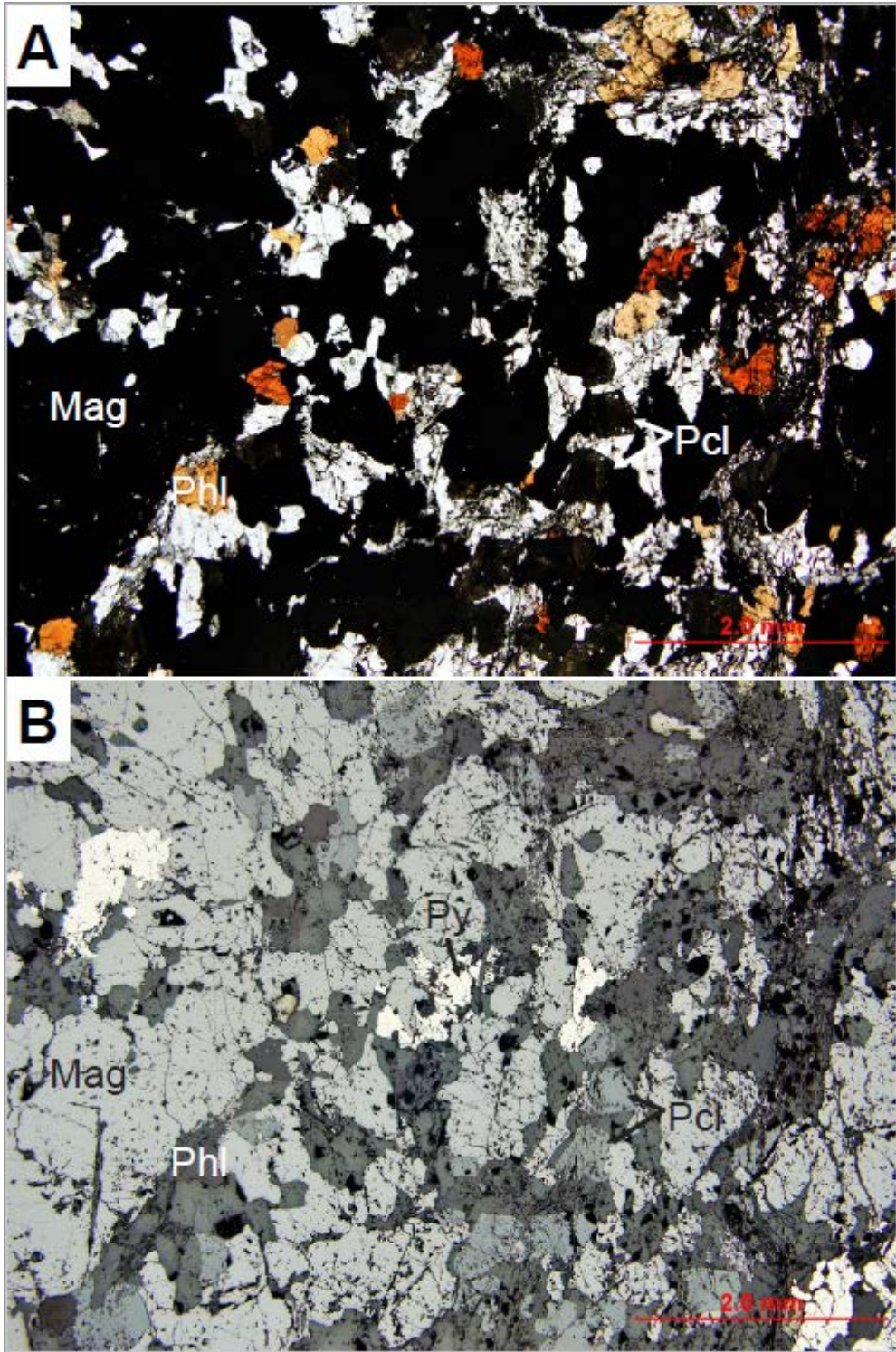
732 Fig. 1. Simplified geological map of the Saint-Honoré alkaline complex (modified from
733 Vallières et al., 2013). The economically Nb-bearing unit is the dolomitic carbonatite unit.



734

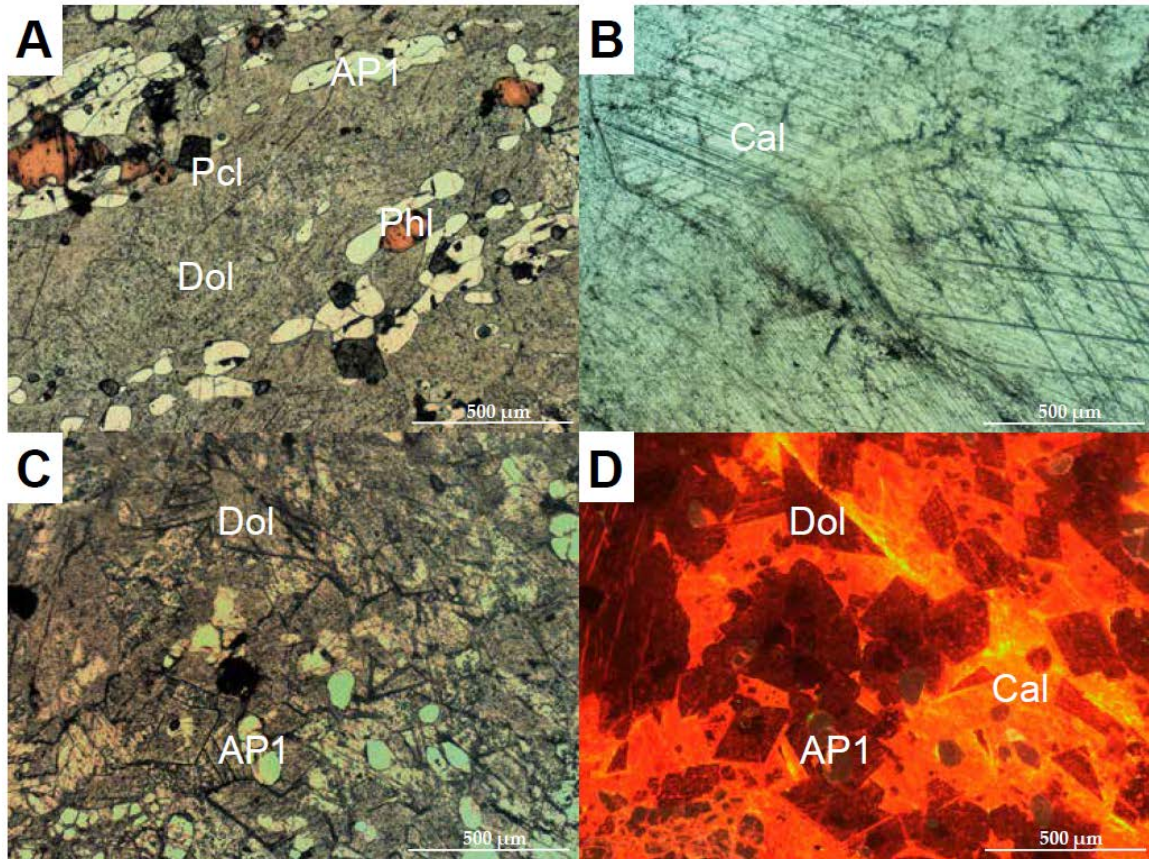
735 Fig. 2. Underground views of mineralized zones. (A) Dolomitic matrix with mineralized
 736 bands of varying size. Late injections of dolomite with late stage apatite (red) cross-cut the

737 unit. (B) A late fine-grained apatite vein cross-cuts the banded mineralized carbonatite (AP:
738 apatite, Mag: magnetite, Phl: phlogopite, Py: pyrite, Pcl: pyrochlore).

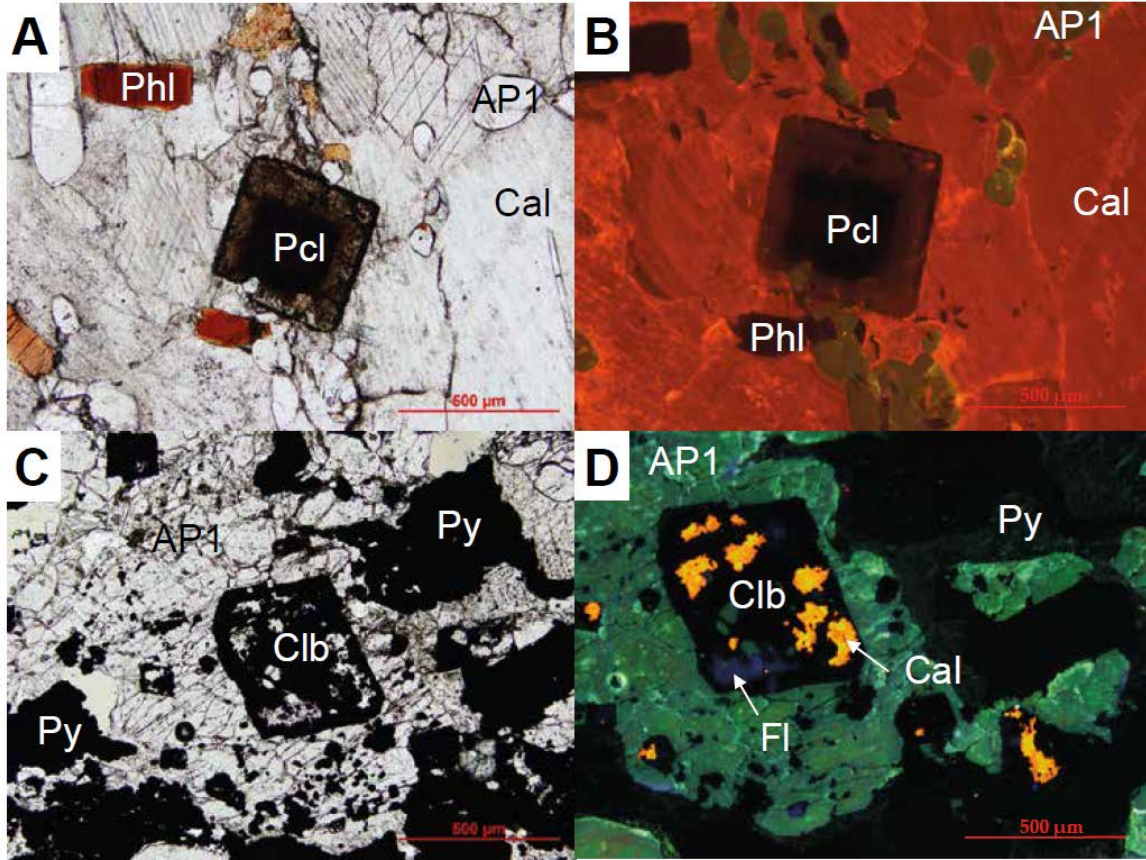


739

740 Fig. 3. Polarized light (A) and reflected light (B) images of a lens of accessory minerals,
741 including magnetite, phlogopite and pyrite in association with apatite and a few pyrochlore
742 grains (Mag: magnetite, Pcl: pyrochlore, Phl: phlogopite, Py: pyrite).



743
744 Fig. 4. A) Polarized light image of altered dolomite (Dol; grayish) with accessory minerals
745 (AP1, Phl and Pcl). (B) Coarse-grained calcite (Cal) with apparent single and losangic
746 cleavages. Polarized (C) and cathodoluminescence (D) images of hydraulic fracturing of
747 dolomite by calcite. (Pcl: pyrochlore, Phl: phlogopite, AP1: apatite).

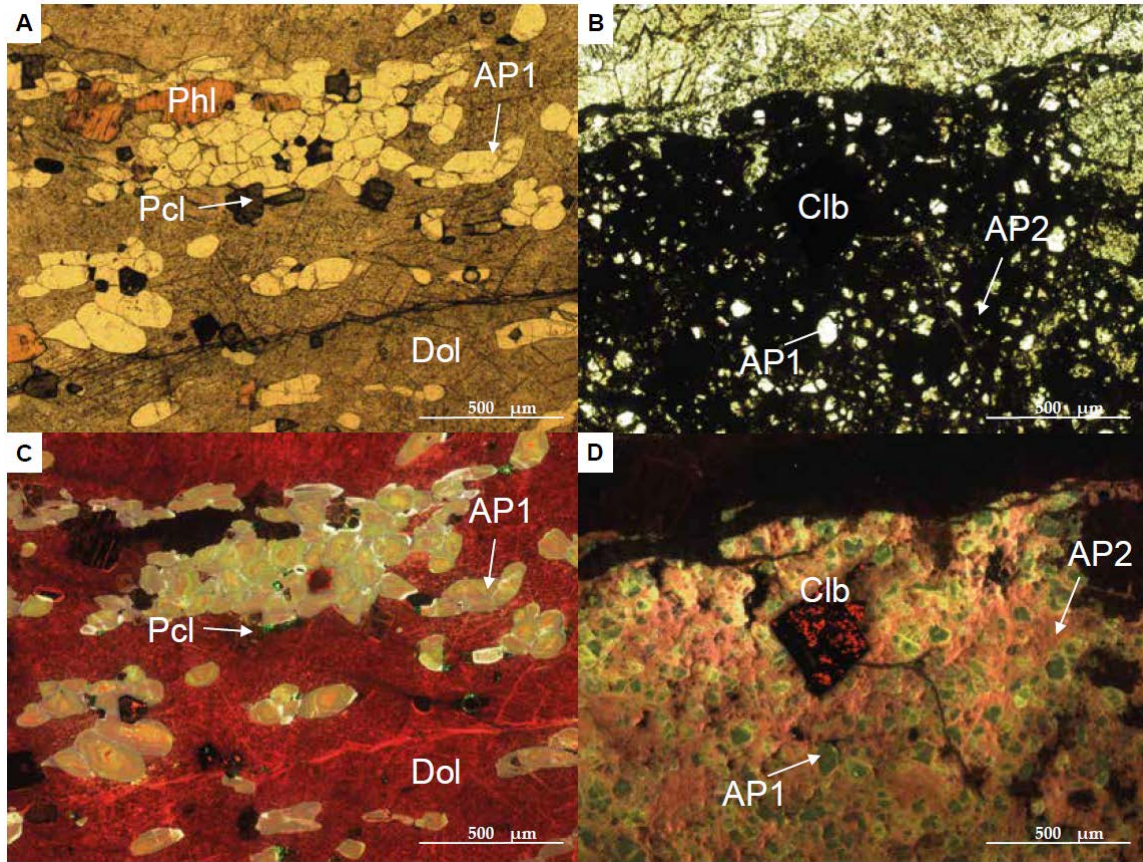


748

749 Fig. 5. Images of euhedral pyrochlore under polarized light (A) and cathodoluminescence

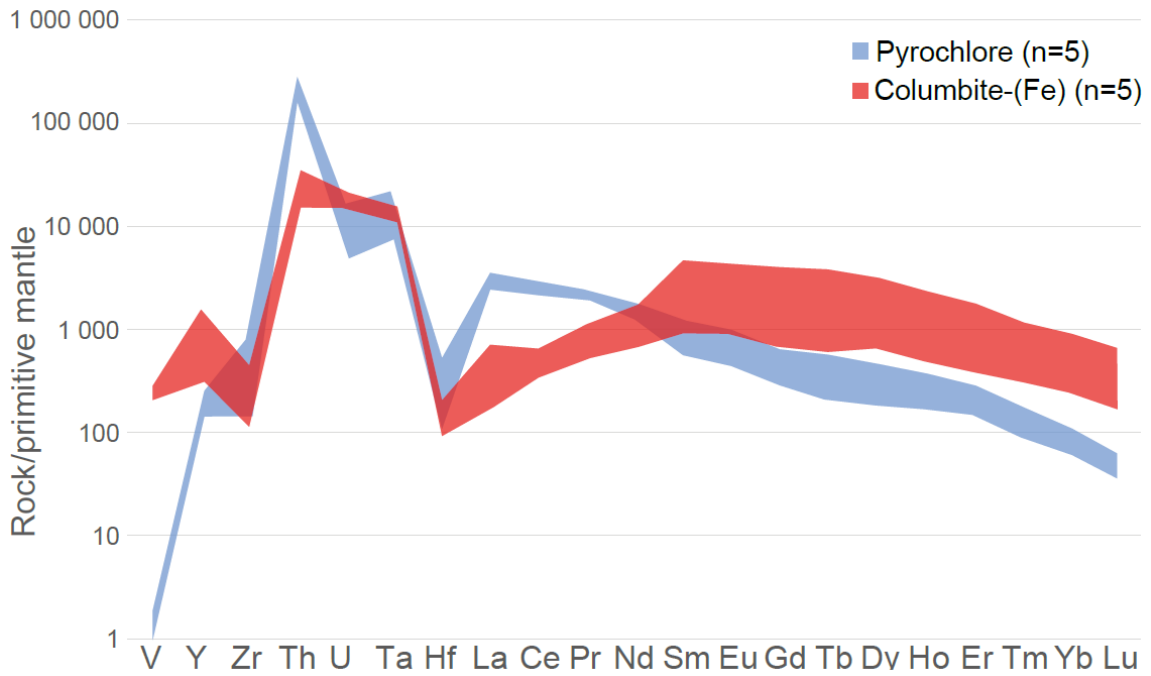
750 (B). Images of anhedral columbite-(Fe) with calcite and fluorite inclusions columbite-(Fe);

751 under polarized light (C) and cathodoluminescence (D).



752

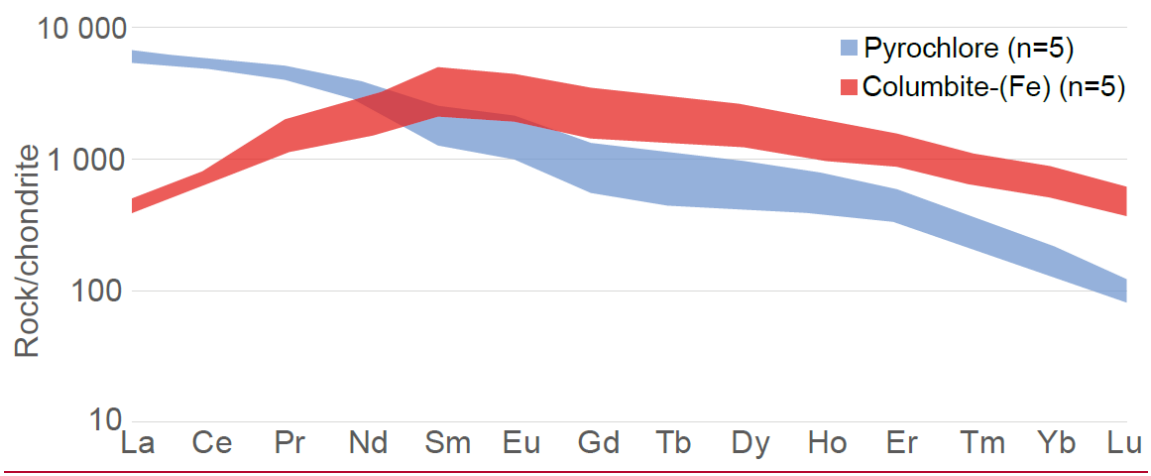
753 Fig. 6. Euhedral pyrochlore associated with a magmatic apatite (AP1) cluster and accessory
 754 minerals: under polarized light (A) and cathodoluminescence (C). Columbite-(Fe)
 755 associated with dark orange apatite (AP2) altering carbonates: under polarized light (B)
 756 and cathodoluminescence (D). (Dol: dolomite, Phl: phlogopite, Py: pyrite, Pcl: pyrochlore,
 757 Clb: columbite-(Fe)).



758

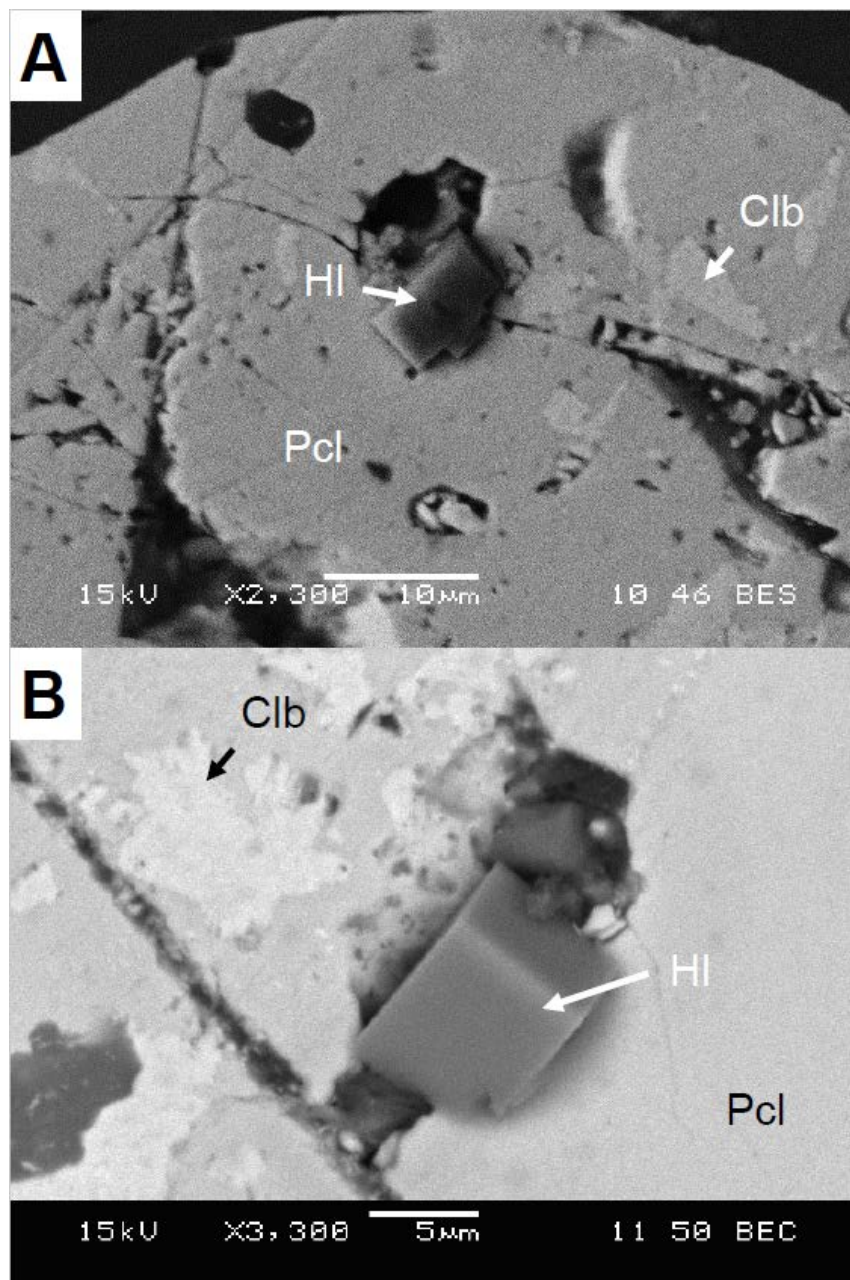
759 Fig. 7. Primitive mantle-normalized trace elements in pyrochlore and columbite-(Fe) from
 760 the Saint-Honoré carbonatite. A considerable increase in V and Y is apparent. Data
 761 obtained from LA-ICP-MS analysis.

762



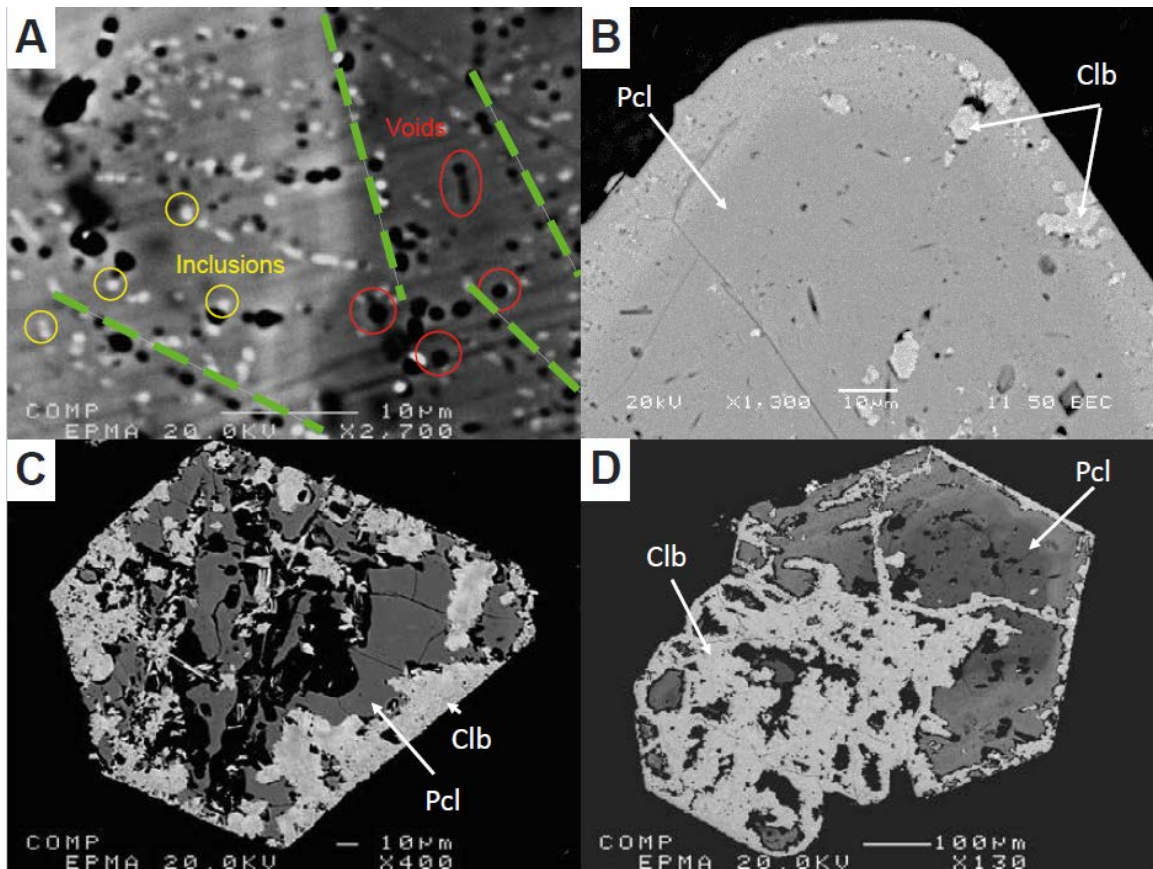
763

764 Fig. 8. Chondrite-normalized REE contents in pyrochlore and columbite-(Fe) from the
765 Saint-Honoré carbonatite. Columbite-(Fe) have a decreased content in LREEs, but is
766 enriched in HREEs compared to pyrochlore. Data obtained from LA-ICP-MS analysis.



767
768 Fig. 9. Microprobe (A) and SEM (B) images of halite (HI) grains in weakly altered
769 pyrochlores (Pcl). Note that halite is crystallizing within irregular-shaped pores. Halite was

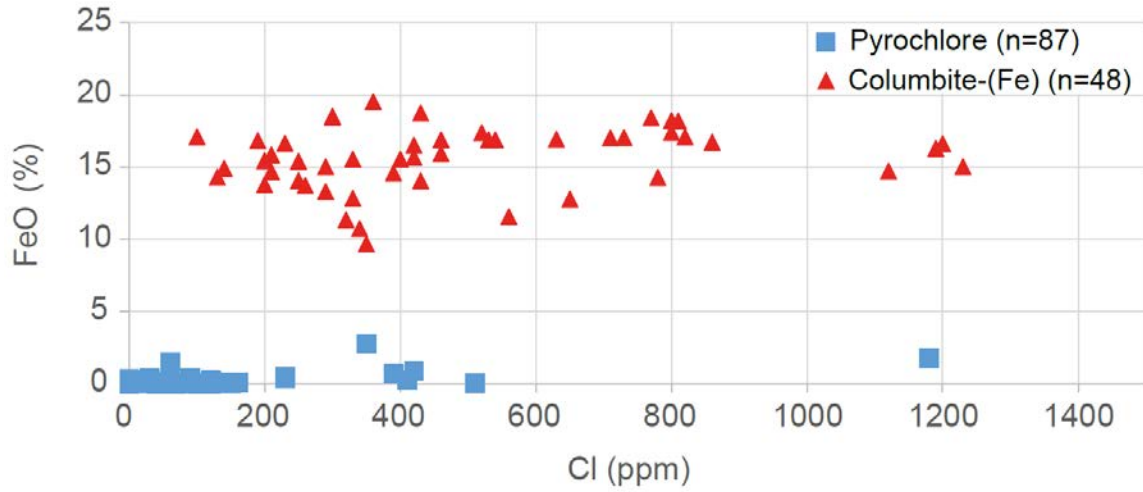
770 only observed in weakly altered pyrochlore (having lost some Na) and was not observed
771 in strongly altered pyrochlore or in columbite-(Fe). Clb: columbite-(Fe).



772

773 Fig. 10. Stages of pyrochlore alteration. (A) Microprobe image of microscopic pores in
774 weakly altered pyrochlore (Pcl). (B) SEM backscatter image of columbitization of a
775 pyrochlore on grain margins. (C) and (D) microprobe images of pyrochlores altering into
776 columbite-(Fe) (Clb) along fractures and grain margins.

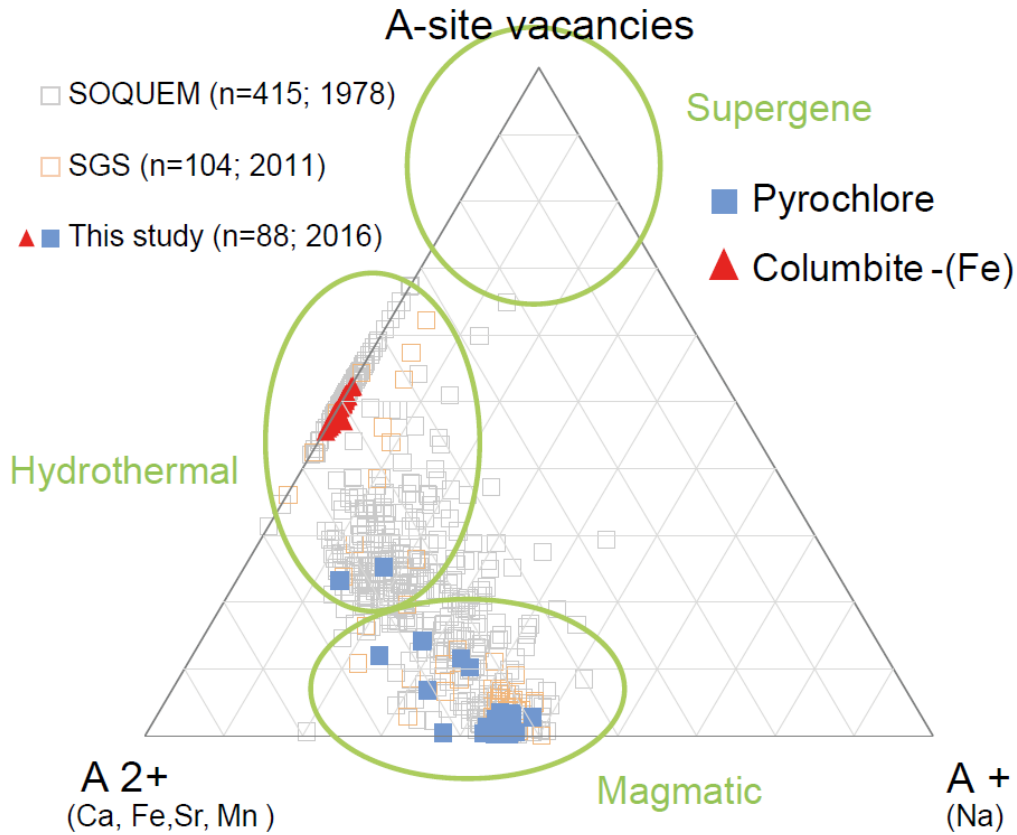
777



778

779 Fig. 11. Microprobe results showing the relationship between % FeO/Cl (ppm) content of
 780 pyrochlore and columbite-(Fe) from the Saint-Honoré carbonatite. The iron content is used
 781 to discriminate the pyrochlore from columbite-(Fe).

782



783

784 Fig. 12. Representation of pyrochlore and columbite-(Fe) within a ternary diagram of major
 785 A-site cations (monovalent and divalent) and vacancies, based on 607 samples. Unaltered
 786 pyrochlores are distributed in the magmatic field whereas strongly altered pyrochlores and
 787 columbite-(Fe) are in the hydrothermal field.

Table 1: Representative major elements (wt%) of unaltered and altered fluorcalciopyrochlore from the Saint-Honoré carbonatite.

Wt. %	Unaltered pyrochlore				Altered pyrochlore		
	S11-C2-core	S01-C2	S07-C2	S07-C3	S21-C10	S05-C2-rim	S05-B
Na ₂ O	7.549	7.274	7.952	7.956	0.031	0.033	0.035
CaO	16.503	16.973	16.162	16.372	4.833	9.229	7.013
SrO	0.690	0.769	0.868	0.864	0.049	0.015	0.062
FeO	0.012	n.d.	0.005	0.102	11.570	6.177	9.671
MnO	n.d.	n.d.	0.008	n.d.	3.585	1.657	2.907
ThO ₂	0.236	0.164	n.d.	0.049	0.289	0.217	0.132
UO ₂	0.010	n.d.	0.029	0.031	n.d.	n.d.	0.032
Y ₂ O ₃	0.069	0.083	0.083	0.094	0.290	1.165	0.302
TiO ₂	2.036	2.827	1.197	1.595	2.304	4.553	2.182
Ta ₂ O ₅	n.d.	n.d.	n.d.	0.029	0.040	0.012	n.d.
Nb ₂ O ₅	69.840	67.697	71.525	70.472	75.896	70.588	75.678
Cl	n.d.	n.d.	0.010	0.008	0.056	0.051	0.035
F	2.753	3.023	3.242	3.348	0.090	n.d.	0.018
-O	1.159	1.273	1.365	1.410	0.038	n.d.	0.008
Total	98.539	97.537	99.716	99.514	98.995	93.697	98.059

Atoms per formula unit calculated on the basis of B=2 cations

Na	0.884	0.862	0.928	0.933	0.003	0.004	0.004
Ca	1.068	1.111	1.042	1.061	0.287	0.560	0.419
Sr	0.024	0.027	0.030	0.030	0.002	-	0.002
Fe ²⁺	0.001	-	-	0.005	0.537	0.292	0.451
Mn	-	-	-	-	0.168	0.079	0.137
Th	0.003	0.002	-	0.001	0.004	0.003	0.002
U	-	-	-	-	-	-	-
Y	0.002	0.003	0.003	0.003	0.009	0.035	0.009
ΣA	1.983	2.005	2.004	2.034	1.010	0.973	1.024
Ti	0.092	0.130	0.054	0.073	0.096	0.194	0.092
Ta	-	-	-	-	0.001	-	-
Nb	1.908	1.870	1.946	1.927	1.903	1.806	1.908
ΣB	2.000	2.000	2.000	2.000	2.000	2.000	2.000
Cl	-	-	0.001	0.001	0.005	0.005	0.003
F	0.526	0.584	0.617	0.640	0.016	-	0.003

Note: n.d. = not detected

Table 2: Representative major elements (wt%) of columbite-(Fe) from the Saint-Honoré carbonatite.

wt. %	Columbite-(Fe)					
	005-C1	011-C3	S11-C1	N47-C1	N22-C3	S21-C3
Na ₂ O	0.041	0.009	0.023	0.006	n.d.	n.d.
CaO	1.490	0.423	1.222	0.636	0.717	0.876
SrO	0.060	0.044	0.040	0.047	0.047	0.032
FeO	16.299	18.421	16.904	17.396	19.540	15.870
MnO	2.702	2.588	3.347	3.407	1.345	4.128
ThO ₂	0.639	0.700	0.453	0.725	0.463	0.130
UO ₂	n.d.	n.d.	0.024	n.d.	0.042	n.d.
Y ₂ O ₃	0.648	0.235	0.111	0.230	0.209	0.191
TiO ₂	2.902	3.652	2.731	2.487	3.405	3.081
Ta ₂ O ₅	0.392	0.178	0.000	0.344	0.155	n.d.
Nb ₂ O ₅	71.714	72.228	73.620	71.089	72.570	74.180
Cl	0.119	0.077	0.046	0.052	0.036	0.021
F	0.000	0.038	0.000	0.070	0.000	0.000
-O	0.000	0.016	0.000	0.029	0.000	0.000
Total	97.006	98.577	98.521	96.460	98.529	98.509

Atoms per formula unit calculated on the basis of six oxygen atoms

Na	0.005	0.001	0.003	0.001	-	-
Ca	0.092	0.026	0.074	0.040	0.043	0.052
Sr	0.002	0.001	0.001	0.002	0.002	0.001
Fe	0.785	0.869	0.800	0.853	0.923	0.740
Mn	0.132	0.124	0.160	0.169	0.064	0.195
Th	0.008	0.009	0.006	0.010	0.006	0.002
U	-	-	-	-	0.001	-
Y	0.020	0.007	0.003	0.007	0.006	0.006
ΣA	1.044	1.037	1.048	1.082	1.045	0.996
Ti	0.126	0.155	0.116	0.110	0.145	0.129
Ta	0.006	0.003	0.000	0.005	0.002	0.000
Nb	1.868	1.842	1.884	1.885	1.853	1.871
ΣB	2.000	2.000	2.000	2.000	2.000	2.000
Cl	0.012	0.007	0.004	0.005	0.003	0.002
F	-	0.007	-	0.013	-	-

Note: n.d. = not detected

Table 3: Trace elements (in ppm) from fluorcalciopyrochlore and columbite-(Fe) samples collected from the Saint-Honoré carbonatite

ppm	Fluorcalciopyrochlore					Columbite-(Fe)				
	004-C4	004-C3	004-C3	004-C2	004-C1	021-C1	021-C2	021-C3	021-C4	021-C5
Cr	n.d.	n.d.	n.d.	n.d.	1	151	328	250	215	42
V	122	75	68	65	74	15 960	19 490	19 560	18 490	18 780
Al	990	1 302	1 341	751	1 310	990	1 120	1 720	2 490	610
Si	2 060	2 090	2 360	3 140	2 480	2 100	1 390	2 590	2 930	926
K	123	92	82	126	44	96	67	108	134	66
Y	623	482	461	817	592	1 016	2 190	5 090	1 530	1 407
Zr	2 040	709	486	3 260	2 970	399	1 557	1 696	536	1 083
Th	12 480	15 340	15 560	13 690	10 450	922	1 849	1 977	1 469	2 115
U	87	95	81	98	248	256	301	253	355	196
Ta	238	325	300	312	629	321	415	435	233	455
Hf	66	30	23	119	106	20	57	66	22	42
La	1 309	1 567	1 589	1 408	1 277	106	92	87	113	324
Ce	3 124	3 376	3 490	3 433	2 974	471	512	546	477	783
Pr	422	451	462	474	371	104	169	208	149	205
Nd	1 503	1 530	1 582	1 780	1 258	652	1 268	1 681	1 003	1 280
Sm	284	257	265	375	188	311	738	1 360	511	540
Eu	89	78	81	120	56	108	249	512	166	179
Gd	189	163	168	263	110	286	691	1 560	476	457
Tb	29	24	24	40	16	47	106	274	77	64
Dy	171	137	138	237	102	302	641	1 650	480	370
Ho	32	25	25	43	21	53	108	274	82	62
Er	71	55	53	94	53	133	249	596	188	140
Tm	7	5	5	9	6	16	27	61	22	16
Yb	30	22	20	36	30	91	142	303	114	82
Lu	3	2	2	3	3	11	15	32	12	9

Note: n.d. = not detected